THE JOURNAL OF BIOLOGICAL CHEMISTRY VOL. 283, NO. 23, pp. 16178–16186, June 6, 2008

ATP-binding Cassette A1-mediated Lipidation of Apolipoprotein A-I Occurs at the Plasma Membrane and Not in the Endocytic Compartments*[S]

Received for publication, November 26, 2007, and in revised form, March 5, 2008 Published, JBC Papers in Press, April 1, 2008, DOI 10.1074/jbc.M709597200

Maxime Denis[1], **Yves D. Landry**[2], **and Xiaohui Zha**[3]

From the Ottawa Health Research Institute, and Department of Biochemistry, Microbiology and Immunology, University of Ottawa, Ontario K1Y 4E9, Canada

ATP-binding cassette transporter (ABC) A1 is required for the lipidation of apolipoprotein A-I to generate high density lipoprotein (HDL). This process is proposed to occur through a retro-endocytosis pathway in which apoA-I internalizes with ABCA1 and generates HDL from the endosomal compartments before resecretion. The aim of this study was to determine the route of apoA-I endocytosis and whether endocytosis contributes to HDL biogenesis. Using confocal microscopy, we found that internalized apoA-I only transiently colocalized with transferrin, a retro-endocytosis marker. Instead, apoA-I perfectly colocalized with a bulk phase uptake marker (fluorescein isothiocyanate-dextran) and, at later time points, with LysoTracker in several cell models including macrophages, fibroblasts, and baby hamster kidney cells. ABCA1 colocalized poorly with internalized apoA-I. To determine the contribution of internalized apoA-I to HDL biogenesis, we specifically removed apoA-I from the cell surface and analyzed the fate of internalized apoA-I. We found that 23% of cell-associated apoA-I was internalized at steady state. Of internalized apoA-I, only 20% was converted to HDL, and the rest was degraded, consistent with a lysosomal destination. We also found that apoA-I was released approximately five times faster from the plasma membrane than from the intracellular compartments. From these kinetic parameters, we estimated that ~5.6% of apoA-I that interacts with cells is degraded and that internalized apoA-I contributes to ~1.4% of total HDL production. We also found that blocking endocytosis with sucrose or cytochalasin D did not decrease cholesterol efflux or HDL biogenesis. We therefore conclude that the plasma membrane is the main platform where ABCA1-mediated lipidation of apoA-I occurs.

Identification of the genetic defect causing Tangier disease has revealed that the ATP-binding cassette transporter A1 (ABCA1)[4] plays a key role in the biogenesis of HDL (1–4). Mutated ABCA1 transporters fail to mediate lipid efflux to extracellular receptors, such as apolipoprotein A-I (apoA-I). This results in the hypercatabolism of apoA-I and a dramatic reduction of plasma HDL levels (5, 6). As a consequence, patients with ABCA1 mutations have an increased risk of developing cardiovascular disease.

The molecular mechanisms by which ABCA1 mediates cholesterol efflux to apoA-I remains elusive. It is hypothesized that ABCA1 may interact with apoA-I and directly transfer lipids onto apoA-I (7, 8). ABCA1 may also facilitate the insertion of lipid-poor apoA-I into the non-raft domains at the plasma membrane, where apoA-I acquires lipids before being released as nascent HDL particles (9). Alternatively, apoA-I has been shown to internalize to the endosomes. It is hypothesized and widely accepted that internalized apoA-I might acquire lipids and be resecreted to the medium as HDL, following the retro-endocytosis pathway (10, 11). The contribution of this retro-endocytosis pathway to the formation of nascent HDL particles, relative to the events occurring at the plasma membrane, remains to be determined. The retro-endocytosis hypothesis is attractive because the endosomes are the second most important reservoir of cellular cholesterol after the plasma membrane (12). By keeping apoA-I transiently in the endosomes, perhaps increasing its local concentration, this pathway may facilitate the transfer of cholesterol to apoA-I. To date, the detailed route by which apoA-I endocytose or exocytose is not known.

Endocytosis of plasma membrane-bound proteins has been extensively described (13). Briefly, receptor-mediated endocytosis refers to a highly efficient process ($t_{1/2}$ = 1–5 min) where adaptors interact with the cytoplasmic tail of cargo proteins and recruit them into clathrin-coated pits (13). Low density lipoprotein and transferrin endocytosis are examples of this process. Endocytosis through clathrin-coated pits represents a highly efficient process such that two-thirds of cargo proteins, *i.e.* transferrin receptors, are found in the endosomes at steady state (14). Another form of endocytosis, bulk phase uptake, refers to a collection of clathrin-independent mechanisms that contribute to the recycling of the plasma membrane (15). Bulk phase uptake is also known to internalize plasma membrane bound proteins although at 5–10% of the rate of receptor-me-

* This work was presented at the American Heart Association Conference held in Orlando, FL, on November 7th 2007. This work was supported by grants from the Canadian Institutes of Health Research, the Canada Innovation Foundation, and the Heart & Stroke Foundation of Canada. The costs of publication of this article were defrayed in part by the payment of page charges. This article must therefore be hereby marked "*advertisement*" in accordance with 18 U.S.C. Section 1734 solely to indicate this fact.
[S] The on-line version of this article (available at http://www.jbc.org) contains supplemental Figs. S1–S4.
[1] Supported by a postdoctoral fellowship from the Canadian Institutes of Health Research.
[2] Supported by an Ontario Graduate Scholarship.
[3] To whom correspondence should be addressed. E-mail: xzha@ohri.ca.

[4] The abbreviations used are: ABC, ATP-binding cassette transporter; apo, apolipoprotein; HDL, high density lipoprotein; FITC, fluorescein isothiocyanate; BHK, baby hamster kidney; DMEM, Dulbecco's modified Eagle's medium; Tf, transferrin.

diated endocytosis (16). The endosomes generated by those respective routes then merge to form the sorting endosomes. From there, most of the membrane and membrane-bound proteins are recycled back to the plasma membrane, whereas the lumen content is delivered to the lysosomes for degradation (13).

apoA-I may endocytose by clathrin-coated pits through its interaction with transmembrane proteins such as ABCA1. The majority of cell-associated apoA-I would then be found in endosomes. This would point toward the endosomal pathway as a major site for apoA-I lipidation. Alternatively, apoA-I could insert into the plasma membrane first and internalize together with slow bulk phase uptake. In that case, the cell-associated apoA-I should be mainly surface-bound, thus implicating the plasma membrane as the dominant location for apoA-I lipidation. We therefore sought to characterize the endocytic route of apoA-I in detail and determine the relative contribution of internalized apoA-I to the biogenesis of nascent HDL particles.

MATERIALS AND METHODS

Cell Culture—All of the cell lines were cultured in DMEM with 10% fetal bovine serum. Baby hamster kidney (BHK) cells stably transfected with noncoding (mock) or an ABCA1-encoding vector were from Dr. Oram (University of Washington, Seattle, WA). ABCA1 expression is under the control of a mifepristone-inducible promoter as previously described (17). Primary human skin fibroblasts of normal and Tangier disease patients (Q597R) were provided by Dr. Genest (McGill University, Montreal, Canada). RAW264.7 mouse macrophages were purchased from ATCC. For induction of ABCA1 expression, the cells were incubated for 20 h with either 10 nM mifepristone (BHK cells), 2.5 μg/ml 22(*R*)-hydroxycholesterol, and 10 μM 9-*cis*-retinoic acid (human skin fibroblasts), or 0.5 mM 8-bromo-cAMP (RAW264.7 macrophages).

Preparation of Fluorescent and Radioactive apoA-I—500 μg of human purified apolipoprotein A-I obtained from Biodesign (Saco, ME) was conjugated to Cy3.5 following the manufacturer's protocol or with 2 mCi ^{125}I (GE-Healthcare/Amersham Biosciences) in the presence of Iodogen® beads (Pierce), purified using a Sephadex G25 column, and extensively dialyzed against phosphate-buffered saline.

Confocal Microscopy—The cells cultured in 35-mm glass-bottomed dishes were incubated with Cy3.5-apoA-I (5 μg/ml) in DMEM alone or plus either AlexaFluor488-Tf (10 μg/ml), FITC-dextran (5 mg/ml) or LysoTracker (0.1 μM) for the indicated times before fixation with 4% paraformaldehyde. Confocal microscopy images were taken using a C1 confocal module on a Nikon TE2000-E inverted fluorescent microscope with a 60× objective and laser lines at 488 and 594 nm. Images from ABCA1 and mock cells were taken under identical conditions. Colocalization was evaluated by counting overlapping intracellular vesicles (250–800 dots/time point) in both channels.

Stripping of Surface-bound apoA-I—The cells were pulse-labeled with either 5 μg/ml Cy3.5-apoA-I or ^{125}I-apoA-I for the indicated times. Following medium removal and wash, the cells were incubated with sucrose (250 mM) in DMEM containing 25 μg/ml unlabeled apoA-I twice for 5 min at 37 °C. This was followed by two washes with phosphate-buffered saline before incubation with chase medium for the indicated times. The cells were then either fixed for microscopy or lysed in 0.5 N NaOH prior to γ-counting. Lower temperatures (15 or 4 °C) did not allow significant cell surface stripping (data not shown).

Cholesterol Efflux—BHK cells were labeled with 2 μCi/ml [^{3}H]cholesterol for 24 h, induced with 10 nM mifepristone, and incubated with 5 μg/ml apoA-I or Cy3.5-apoA-I. At the end of the efflux period, the medium was collected, and the cells were lysed in 0.5 N NaOH. Radioactivity in the medium and cells was determined by scintillation counting, and the efflux was calculated as the percentage of $CPM_{med}/(CPM_{med} + CPM_{cell})$.

^{125}I-apoA-I Cell Association—For dose-response experiments, induced BHK cells were incubated for 2 h with the indicated doses of ^{125}I-apoA-I in DMEM. For time course experiments, the cells were incubated for the indicated times with 5 μg/ml ^{125}I-apoA-I. The nonspecific association was determined by identical procedure with the labeling medium containing 200 μg/ml of unlabeled apoA-I. At the end of the incubation, the cells were lysed with 0.5 N NaOH and counted to determine whole cell association. Alternatively, to determine intracellular cell association, surface-bound ^{125}I-apoA-I was stripped prior to γ-counting. Protein concentration was determined by the Lowry method, and specific association was determined by subtracting nonspecific counts from total counts for each point. The plasma membrane association was calculated by subtracting the specific intracellular association from the specific whole cell association. Kinetic parameters (K_d, B_{max}, K_{on}, K_{off}, $t_{1/2}$) were determined using GraphPad Prism 4.0 software.

Precipitation with Trichloroacetic Acid on the Chase Medium—Intact protein precipitation was performed for 1 h on ice in chase medium by adding ice-cold sodium deoxycholate (final concentration, 0.15%) followed by ice-cold trichloroacetic acid (final concentration, 10%) before centrifugation at 13,000 × *g*. The supernatants (degraded) and pellets (intact protein) were counted.

Two-dimensional Gel Electrophoresis of Nascent HDL Particles—The media were concentrated by ultrafiltration (Amicon Ultra; molecular weight cut-off, 10,000; Millipore). The samples (300 μl) were loaded on a 1.5-mm-thick 0.75% agarose gel prepared in Tris-glycine buffer, pH 8.3, using 10% polyacrylamide to seal the bottom of the gel as described previously (18). The second dimension, a 4–22.5% polyacrylamide nondenaturing concave gradient gel, was run at 4 °C for 24 h at 10 mA/gel, as previously described (19). After transfer (30 mA, 24 h, 4 °C) onto nitrocellulose membranes, molecular weight markers were revealed by Ponceau S. The membranes were either directly revealed by autoradiography or processed for immunoblotting.

RESULTS

Endocytosis of apoA-I in ABCA1-expressing cells has been previously reported (11, 20), but the specific route has yet to be clarified. To do so, we fluorescently (Cy3.5) labeled apoA-I and tested whether Cy3.5-apoA-I is a valid analog of native apoA-I. We found that Cy3.5 apoA-I behaves identically to native apoA-I in terms of the specificity of cell association (supplemental Fig. S1, *A* and *B*), the ability to promote cholesterol

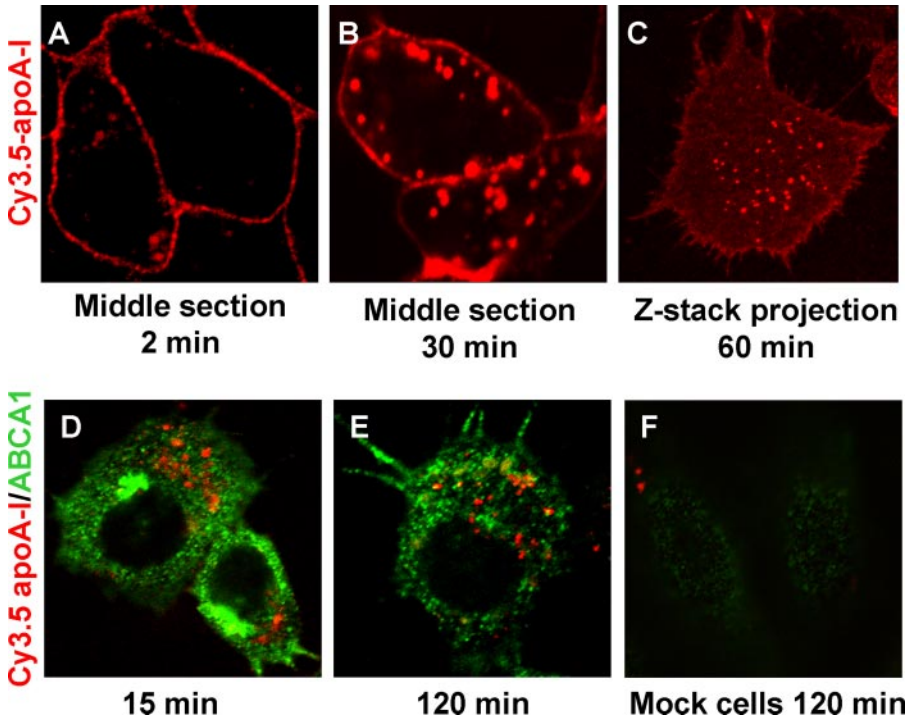

FIGURE 1. **Association and internalization of Cy3.5-apoA-I in BHK cells.** ABCA1-expressing BHK cells were incubated with 5 μg/ml Cy3.5-apoA-I for 2 min (*A*) or 30 min (*B*) and analyzed by confocal microscopy. *C*, after a 60-min incubation, serial confocal *z* sections were taken throughout the cellular volume and projected onto one plane to form a single image. *D* and *E*, ABCA1-expressing BHK cells were labeled with 5 μg/ml Cy3.5-apoA-I (*red*) for 5 min and chased for 15 min (*D*) or 120 min (*E*). The cells were then immunofluorescently stained for ABCA1 (*green*). *F*, mock BHK cells were incubated with Cy3.5-apoA-I for 120 min and then immunostained for ABCA1.

efflux (supplemental Fig. S1*D*), and the capacity to generate nascent HDL particles (supplemental Fig. S1*C*) in BHK cells expressing ABCA1. Similar results were obtained using primary human skin fibroblasts from control and Tangier subjects (data not shown).

We then used Cy3.5-apoA-I to track apoA-I endocytosis over time by confocal microscopy. Cy3.5-apoA-I bound to the plasma membrane first (Fig. 1*A*, 2 min) and then gradually appeared in the intracellular organelles (Fig. 1*B*, 30 min). *z* sections that covered the entire cell volume revealed that the majority of cell-associated Cy3.5-apoA-I was localized to the plasma membrane at 60 min, whereas a small fraction was internalized in punctated structures (Fig. 1*C*). This is in agreement with previous observations obtained by cell surface biotinylation in a different cell model (21). We also examined whether apoA-I was internalized with ABCA1. The cells were pulsed with Cy3.5-apoA-I for 5 min and chased for up to 2 h before immunofluorescent detection of ABCA1. We found little colocalization (<10%) between Cy3.5-apoA-I and ABCA1 throughout the chase, consistent with recent reports showing that the majority (~90%) of cell-associated apoA-I is not bound to ABCA1 (22). Representative images are shown in Fig. 1 (*D–F*).

We next investigated the route of apoA-I endocytosis. We postulated that, if apoA-I is internalized through the clathrin-coated pits and is recycled back to the extracellular medium, it should colocalize at all times with transferrin (Tf), a well established marker for this pathway. The cells were pulse-labeled for 5 min with Cy3.5-apoA-I (5 μg/ml) and chased in apoA-I-free medium for up to 2 h. The recycling pathway was tracked by Alexa488-Tf. At the end of the chase, the cells were fixed and analyzed by confocal microscopy. At early time points, most of the apoA-I was found in Tf-containing compartments (Fig. 2*A*, *upper panels*, 15 min), indicating the passage of apoA-I through the endosomal system. At later time points, however, the colocalization observed between Tf and apoA-I was much less (Fig. 2*A*, *upper panels*, 120 min), suggesting the departure of apoA-I from the recycling pathway. This observation was further confirmed when we scored a large number of Cy3.5-apoA-I-positive organelles (>500 organelles/time point) for the presence of Alexa488-Tf in the same compartment. Although most of the Cy3.5-apoA-I-positive compartments contained Tf (~100%) at $t \leq$ 1 h, the number gradually decreased to less than 40% at later time points, indicating that apoA-I was diverted from the recycling pathway (Fig. 2*A*, *lower panel*). It is worth noting that, even though Tf was present in all apoA-I-positive compartments at the early time points, a large number of Tf-positive compartments did not have apoA-I (Fig. 2*A*, *upper panels*, 15 min). This further suggests that apoA-I only shared a part of the recycling pathway with Tf.

To test whether apoA-I is internalized by bulk phase uptake, we coincubated Cy3.5-apoA-I with FITC-dextran, a bulk phase marker, for up to 2 h and examined their localizations by confocal microscopy. We found that there was perfect colocalization between internalized Cy3.5-apoA-I and FITC-dextran at all time points (Fig. 2*B*, *upper panels*). Quantitatively, nearly all Cy3.5-apoA-I-positive compartments contained FITC-dextran (Fig. 2*B*, *lower panel*). In contrast to Tf, all FITC-dextran-positive compartments were also positive with Cy3.5-apoA-I (Fig. 2*B*, *upper panels*). This strongly indicates that apoA-I was internalized through bulk phase uptake, most likely by being bound to the plasma membrane. Bulk phase uptake can also internalize apoA-I from the medium, but this process was negligible because ABCA1$^{-/-}$ cells do not take up a measurable amount of apoA-I (Fig. 1*F*) despite enhanced endocytosis in these cells (23).

Because FITC-dextran is known to reach lysosomes at later time points, this raised the possibility that internalized apoA-I may be targeted to lysosomes. We therefore prelabeled the lysosomes with LysoTracker-Green. The cells were then pulse-labeled with Cy3.5-apoA-I for 5 min and chased in Cy3.5-apoA-I free medium for up to 6 h. There was little colocalization between apoA-I and LysoTracker at early time points, as expected (Fig. 2*C*, 15 min). However, by 2 h, the majority of

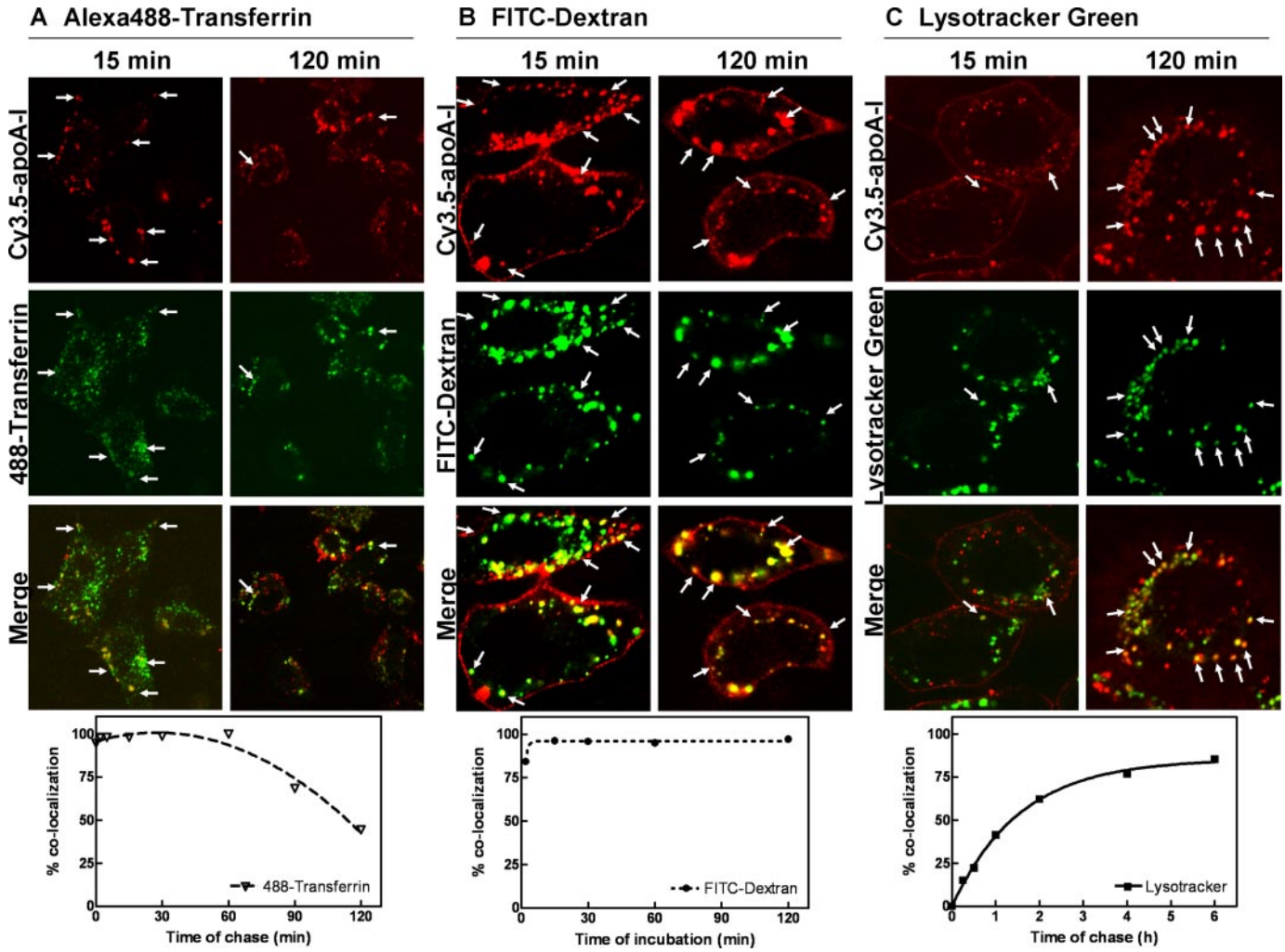

FIGURE 2. **Determination of the Cy3.5-apoA-I endocytic route.** ABCA1-expressing BHK cells were: coincubated with 5 μg/ml Cy3.5-apoA-I and 20 μg/ml Alexa488-transferrin for 2 min, washed, and chased for up to 2 h (*A*); continuously incubated with 5 μg/ml Cy3.5-apoA-I and 5 mg/ml FITC-dextran for up to 2 h (*B*); or preincubated with 0.1 μM LysoTracker Green for 15 min, pulse coincubated with 5 μg/ml Cy3.5-apoA-I and LysoTracker Green for 5 min, and chased in DMEM containing LysoTracker Green for up to 6 h (*C*). *Upper panels*, internalized Cy3.5-apoA-I-containing vesicles were analyzed by confocal microscopy for colocalization with the respective green labels. The images are shown for 15- and 120-min time points. The *arrows* indicate representative colocalizing points. *Bottom panels*, percentage of colocalization represents the percentage of apoA-I-positive compartments that also contain Tf or FITC-dextran or LysoTracker. Approximately 250–800 dots were analyzed for each time point for all three experiments.

Cy3.5-apoA-I was seen to colocalize with LysoTracker (Fig. 2*C*, 2 h), suggesting that apoA-I had reached the lysosome. Scoring a large number of Cy3.5-apoA-I-positive compartments for the presence of LysoTracker indicted a gradual appearance of apoA-I in the LysoTracker-positive compartments (Fig. 2*C*, *lower panel*), consistent with apoA-I being delivered to the lysosomes.

Cy3.5 fluorescent modification of apoA-I could potentially trigger its lysosomal targeting. To explore this possibility, we incubated cells with unlabeled apoA-I along with LysoTracker Red for 1 h. apoA-I was detected by immunofluorescent staining. Native apoA-I decorated the plasma membrane as well as intracellular compartments, similar to Cy3.5-apoA-I. Importantly, these intracellular compartments colocalized extensively with Lysotracker (supplemental Fig. S2*A*). Fluorescent modification therefore could not be the cause of apoA-I targeting to lysosomes. We then investigated whether internalized apoA-I was targeted to the lysosome in other cell types that express endogenous ABCA1. We found that in a mouse macrophage cell line (RAW264.7), Cy3.5-apoA-I almost perfectly colocalized with LysoTracker (supplemental Fig. S2*B*). Similar results were obtained in normal human skin fibroblasts, RAW macrophages, and HepG2 hepatocytes (supplemental Fig. S2*C*). In contrast, mock transfected cells, uninduced RAW, and human skin fibroblasts, as well as skin fibroblasts from a Tangier patient, failed to bind and internalize Cy3.5-apoA-I. This suggests that lysosomal targeting of internalized apoA-I is a general phenomenon operating in ABCA1-expressing cell models.

Lysosomes are best known for their role in degradation, although apoA-I is not known to be significantly degraded in most cell types. Interestingly, recent studies have shown that lysosomes may also fuse with the plasma membrane and release their contents to the extracellular medium (24). In addition, apoA-I was reported to shuttle from late endosomes back to the cell surface (10). We therefore wanted to quantitatively examine the fate of internalized apoA-I and, in particular, to determine the relative contribution of apoA-I internalization to the

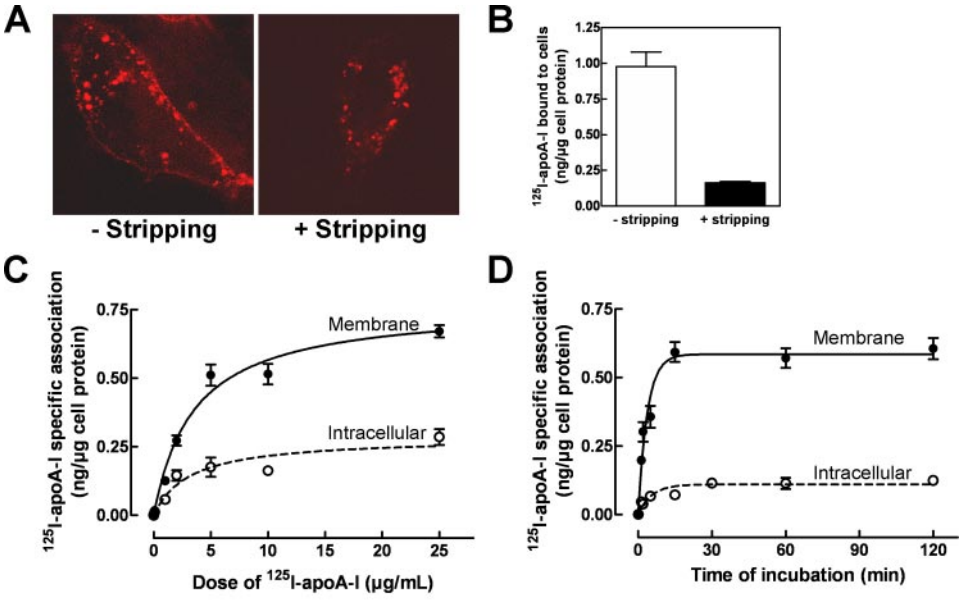

E

ApoA-I/cell association	$_{app}$Kd (µg/mL)	$_{app}$Bmax (ng/µg cell protein)	K_{on} (min^{-1})	Approx. t½ (min)
Whole cells	3.37 ± 0.44	1.05 ± 0.05	0.26 ± 0.02	2.6
Plasma membrane	3.53 ± 0.43	**0.77 ± 0.03**	0.27 ± 0.02	2.6
Intracellular	3.14 ± 0.76	**0.28 ± 0.02**	0.18 ± 0.01	3.8

FIGURE 3. **apoA-I association with cellular compartments.** ABCA1-expressing BHK cells were labeled with either 5 µg/ml Cy3.5-apoA-I for 30 min (*A*) or ^{125}I-apoA-I for 2 min (*B*). The cells were then washed with 250 mM sucrose in DMEM containing 25 µg/ml unlabeled apoA-I at 37 °C. The cells were either analyzed by confocal microscopy (*A*) or quantified for cell-associated ^{125}I-apoA-I before and after stripping (*B*). *C*, cells were incubated with increasing doses of ^{125}I-apoA-I for 2 h. Cell-associated ^{125}I-apoA-I was quantified directly or after stripping. ^{125}I-apoA-I association with whole cells (without stripping), intracellular compartments (after stripping), or plasma membrane (whole cells minus intracellular compartments) was then determined. The data represent the means ± standard deviation of specific ^{125}I-apoA-I association obtained from triplicate wells. *D*, cells were incubated with 5 µg/ml ^{125}I-apoA-I for indicated times. The cells were then processed as described in *C*. *E*, kinetic analysis of *C* and *D* for whole cells, plasma membrane, and intracellular compartments.

overall biogenesis of HDL. To do so, we needed to develop a method to specifically quantify the amount of apoA-I associated with the intracellular compartments by removing apoA-I from the cell surface. Acid washing, a classic method to strip off cell surface-bound ligands including Tf, was found without effect on cell surface-bound Cy3.5-apoA-I (not shown). In a second approach, we successfully stripped off cell surface Cy3.5-apoA-I with excess unlabeled apoA-I in the presence of sucrose. Sucrose was necessary to prevent all types of endocytosis during 5 min of stripping (supplemental Fig. S3). Cell surface Cy3.5-apoA-I could only be efficiently replaced by unlabeled apoA-I at 37 °C. By confocal microscopy, we observed a complete removal of surface-bound Cy3.5-apoA-I without affecting the intracellular pool (Fig. 3*A*). High stripping efficiency was further confirmed with ^{125}I-apoA-I. In cells pulse-labeled with ^{125}I-apoA-I for 2 min, a condition where apoA-I was mostly seen on the plasma membrane with relatively minor endocytosis (Fig. 1*A*), the stripping protocol removed more than 80% of cell-associated ^{125}I-apoA-I (Fig. 3*B*). The residual radioactivity was partially due to a minor degree of endocytosis during 2 min of pulse. We therefore applied this protocol to a dose-response experiment to quantify the specific ^{125}I-apoA-I association with the different cellular pools: whole cells (no stripping), intracellular compartments (after stripping), and plasma membrane (whole cells minus intracellular compartments) (Fig. 3*C*). We found that the plasma membrane and intracellular compartments have a similar affinity for apoA-I (Fig. 3*E*, $_{app}Kd$). Further analysis of apparent B_{max} values, however, revealed that the plasma membrane has approximately a three times greater capacity to accommodate apoA-I than the intracellular compartments (Fig. 3*E*, $_{app}Bmax$). In concordance with results shown in Fig. 1*D*, mock cells failed to bind and internalize significant amounts of ^{125}I-apoA-I (not shown). Using a similar approach, we also performed a time course experiment (Fig. 3*D*). We found that ^{125}I-apoA-I rapidly saturated the cell surface, whereas its appearance in intracellular compartments was slightly delayed (Fig. 3*E*, K_{on}). These results also indicated that, at equilibrium, internalized apoA-I represented ~27% of whole cell-associated apoA-I.

The lipidation and the subsequent dissociation of apoA-I from cells is thought to form HDL particles. To evaluate the potencies of the plasma membrane and intracellular compartments to release apoA-I to the medium, we investigated the respective kinetics of dissociation from each compartment. The cells were first incubated for 2 h with ^{125}I-apoA-I to saturate all compartments. Next, plasma membrane ^{125}I-apoA-I was stripped, and the cells were chased in ^{125}I-apoA-I free medium for up to 6 h. The specific radioactivity associated with the whole cells and intracellular compartments was monitored at all time points. The plasma membrane-associated ^{125}I-apoA-I was then calculated (total minus intracellular). As shown in Fig. 4*A*, the specific radioactivity associated with both compartments decreased over time. The dissociation of ^{125}I-apoA-I from the plasma membrane, however, was rapid ($K_{off\,pm} = 0.25 \pm 0.06\ min^{-1}$) compared with the ^{125}I-apoA-I release from intracellular compartments ($K_{off\,intra} = 0.02 \pm 0.01\ min^{-1}$). The slow release of apoA-I from the intracellular compartments was also evident in terms of $t_{½}$ ($t_{½\,pm} = \sim 2.8$ min and $t_{½\,intra} = \sim 38.4$ min). These results, together with results shown in Fig. 3*E*, suggested that the association/dissociation kinetics of apoA-I with the plasma membrane (on and off rates) are much faster than that of intracellular compartments. The residence time of apoA-I at the plasma membrane is therefore likely to be short.

Having shown that internalized apoA-I colocalized with LysoTracker, we next investigated whether internalized apoA-I was significantly degraded. The dissociation medium obtained from stripped cells used in Fig. 4*A* was collected, and the amount of degraded material appearing in the

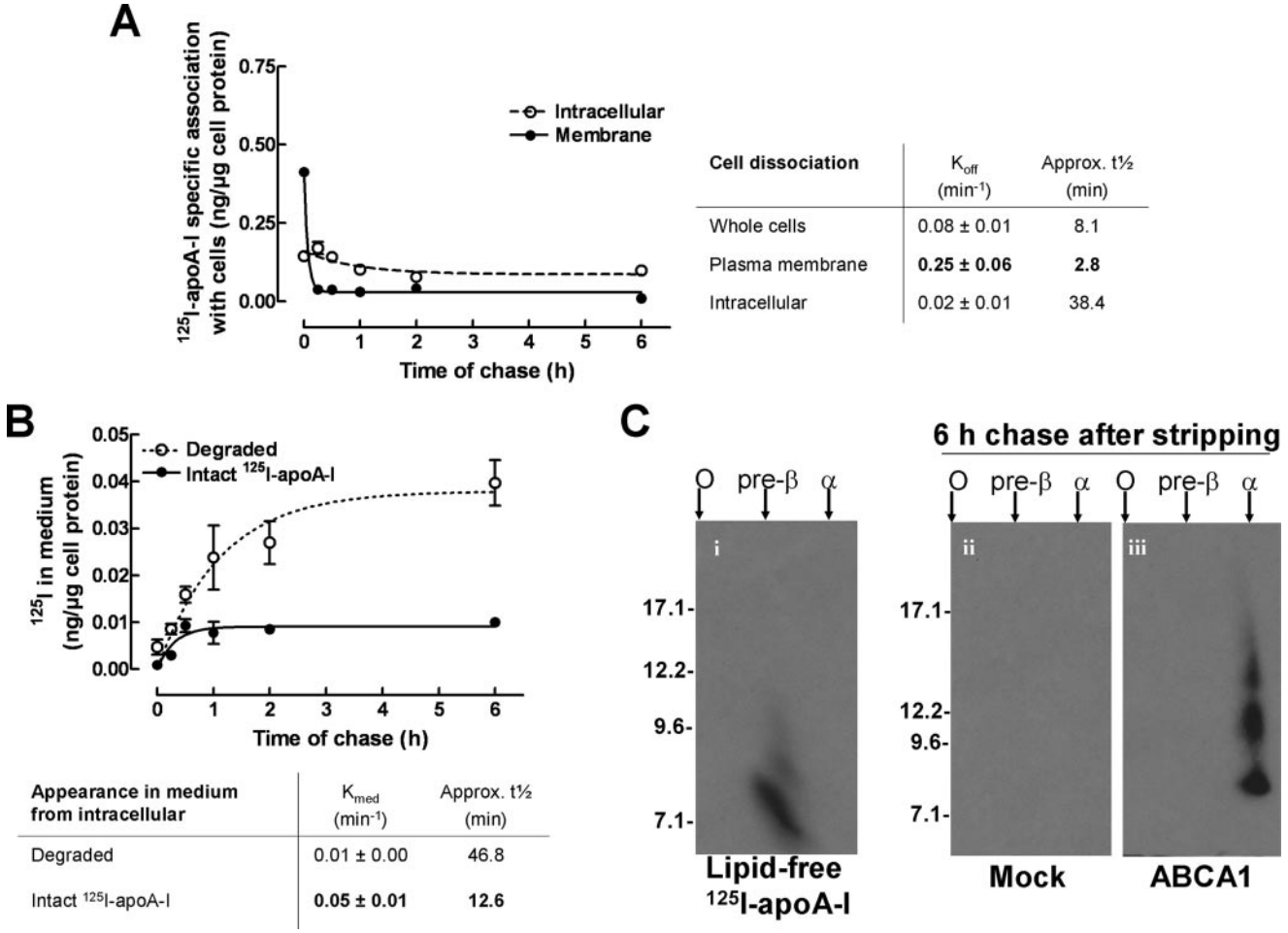

Cell dissociation	K_{off} (min^{-1})	Approx. t½ (min)
Whole cells	0.08 ± 0.01	8.1
Plasma membrane	**0.25 ± 0.06**	**2.8**
Intracellular	0.02 ± 0.01	38.4

Appearance in medium from intracellular	K_{med} (min^{-1})	Approx. t½ (min)
Degraded	0.01 ± 0.00	46.8
Intact ^{125}I-apoA-I	**0.05 ± 0.01**	**12.6**

FIGURE 4. **apoA-I is slowly dissociated from intracellular compartments and released to medium in a degraded form.** *A*, ABCA1-expressing BHK cells were incubated with ^{125}I-apoA-I for 2 h. Surface-bound ^{125}I-apoA-I was either stripped off or not, followed by chase in ^{125}I-apoA-I-free medium for indicated times up to 6 h. Specific ^{125}I-apoA-I radioactivity was determined for whole cells (no stripping), intracellular compartments (with stripping), and plasma membrane (whole cells minus intracellular compartments). *B*, the chase medium from the surface-stripped cells was subjected to trichloroacetic acid precipitation. Degraded and intact ^{125}I-apoA-I were determined from counts in the supernatant and pellet, respectively. For comparison purposes, the radioactivity associated with degraded material was converted to mass of apoA-I equivalents. The data represent the means ± standard deviation of specific ^{125}I-apoA-I association obtained from triplicate wells. *C*, medium collected after a 6-h chase in *B* were subjected to nondenaturing two-dimensional gel electrophoresis. Extensive autoradiography (5 days) was required to detect those particles.

medium was quantified by trichloroacetic acid precipitation. In a separate control experiment, intact ^{125}I-apoA-I was seen to be efficiently precipitated by trichloroacetic acid (>97%). We therefore used this approach to quantify the amount of intact ^{125}I-apoA-I in trichloroacetic acid pellets and the amount of degraded material in trichloroacetic acid supernatants. Fig. 4*B* shows that ~80% of the radioactivity released from the intracellular compartments appeared as degraded product, likely because of lysosomal degradation. The remaining 20% of radioactivity was intact ^{125}I-apoA-I (pellets) and appeared in the medium at a rate of K_{med} = 0.05 ± 0.01 min^{-1} ($t_{½}$ = ~12.6 min), similar to bulk membrane recycling ($t_{½}$ = ~15 min) (25). This suggested that not all internalized apoA-I was targeted for lysosomal degradation. We next determined by two-dimensional nondenaturing gels whether these intact ^{125}I-apoA-I molecules from the intracellular pool are nascent HDL particles. We observed that the intact ^{125}I-apoA-I released from intracellular pools is effectively converted to normal size nascent HDL particles (Fig. 4*C*).

Using the parameters obtained from above, we estimated the extent of degradation and the relative contribution of endosomal recycling to the generation of HDL. Although ~27% of cell-associated apoA-I is intracellular at steady state (Fig. 3*C*), the dissociation rate of apoA-I from the plasma membrane is five times faster than the rate of release of intact apoA-I from intracellular compartments (compare plasma membrane K_{off} values with intact apoA-I K_{med} obtained from Fig. 4). Taking that into account, we deduced the following (Fig. 5). At steady state, for every 100 molecules that interact with whole cells, 73 are bound to the cell surface, whereas 27 are internalized. From those internalized, five (20% of internalized apoA-I) may return to extracellular medium as an intact molecule, whereas the remaining 22 (80%) will be degraded. However, for every cycle of internalization/resecretion, the 73 molecules of apoA-I on the plasma membrane would associate/dissociate approximately five times. The plasma membrane could therefore potentially release 365 molecules of apoA-I (73 × 5 molecules) into the medium for each cycle of internalization/resecretion. Therefore, the apoA-I degradation represents 5.6% of total

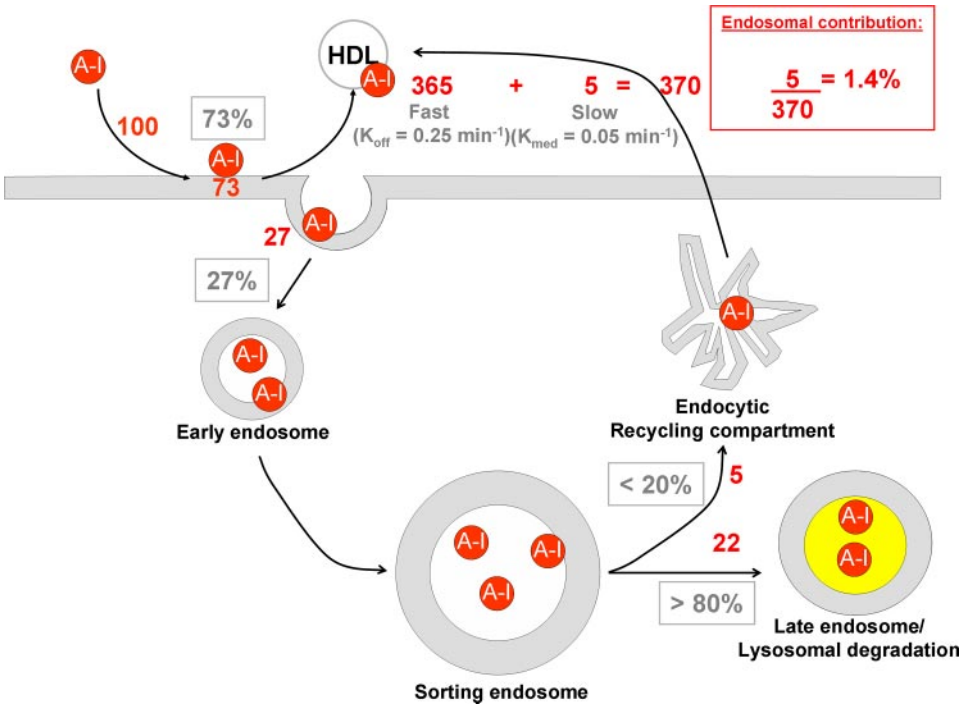

FIGURE 5. **Integrated overview of the relative contribution of cell-associated apoA-I to HDL formation.** A small portion of surface-bound apoA-I (27%) was internalized to the early and then sorting endosomes, during which 80% of apoA-I became dissociated from the endocytosed membrane and therefore was delivered to the late endosomes/lysosomes. 20% of apoA-I that remained associated with the membrane in the sorting endosomes proceeded to the recycling compartment and was released as nascent HDL with $t_{1/2}$ = ~12.6 min (K_{med} = 0.05 min^{-1}). For each cycle of apoA-I endocytosis/recycling, surface-bound apoA-I dissociates five times faster ($t_{1/2}$ = ~2.8 min; K_{off} = 0. 25 min^{-1}) from the plasma membrane and presumably generates HDL. The *numbers* in *red* indicate the estimated contribution of each compartment for 100 molecules interacting with cells.

apoA-I that interacted with cells (22/(27 + 365) molecules), suggesting that lysosomal degradation is a minor process compared with the overall lipidation of apoA-I. More importantly, our calculations indicate that the contribution of resecreted intact apoA-I, relative to the total number of apoA-I molecules converted to nascent HDL particles, is ~1.4% (5/(5 + 365) molecules). We conclude that internalization of apoA-I does not significantly contribute to the formation of nascent HDL particles.

Interestingly, previous studies have employed pharmacological reagents to block endocytosis and found diminished cholesterol efflux to apoA-I (11, 26). We therefore tested two additional reagents known also to inhibit endocytosis. The cells were treated with cytochalasin D, an actin filament-disrupting drug known to acutely and reversibly inhibit endocytosis (27), and this reduced Cy3.5-apoA-I endocytosis by ~80% (Fig. 6, *A* and *B*). Under those conditions, inhibiting endocytosis did not decrease apoA-I-mediated cholesterol efflux (Fig. 6*C*). Similar results were obtained using RAW macrophages induced with 8-bromo-cAMP (supplemental Fig. S4). Two-dimensional gel analysis of the efflux medium further confirmed that blocking endocytosis did not interfere with the generation of α-migrating HDL particles (Fig. 6*D*). Using sucrose (30 min) to block apoA-I endocytosis also failed to decrease [^{3}H]cholesterol efflux or nascent HDL production (data not shown). This suggests that blocking endocytosis does not necessarily inhibit cholesterol efflux or the generation of nascent HDL particles. Interestingly, cytochalasin D also increased the amount of intact ^{125}I-apoA-I found in the medium (Fig. 6*E*), presumably by preventing lysosomal degradation.

DISCUSSION

Here, we have studied the fate of endocytosed apoA-I and its relative contribution to the formation of nascent HDL particles. Pioneering studies by Takahashi and Smith (11) and others (10, 26) showed that apoA-I is internalized and that endocytosed apoA-I shuttles back to the plasma membrane to be resecreted. Our results here largely confirm these observations. A fraction of apoA-I colocalized with Tf-positive compartments even after 2-h chase (Fig. 2*A*, *lower panel*) and indeed was resecreted as HDL particles (Fig. 4*C*). However, when we compared the magnitude of HDL generation from this retro-endocytosis mechanism with the overall HDL production in ABCA1-expressing cells, we found that the retro-endocytosis pathway does not contribute significantly to HDL formation.

Several lines of evidence from our findings point toward the plasma membrane as the primary location of HDL biogenesis. First, we found that most of internalized apoA-I colocalized with the bulk phase uptake marker (Fig. 2*B*) and, by 6 h, ~80% appeared in LysoTracker-positive compartments (Fig. 2*C*), suggesting that very little apoA-I recycles back to the plasma membrane. Second, internalized apoA-I was extensively degraded (80%). Third, and perhaps most importantly, the majority of the apoA-I is on the cell surface (>70%) and is released from the plasma membrane at least five times faster ($t_{1/2\ pm}$ = ~2.8 min) than from endosomal recycling ($t_{1/2\ medium}$ = ~12.6 min). This means that apoA-I on the plasma membrane can be converted to HDL five times faster than resecreted internalized apoA-I. Altogether, these results make the plasma membrane the predominant location where HDL is produced.

Our conclusion that apoA-I internalization plays a minor role in ABCA1-mediated HDL generation is in apparent discrepancy with previous studies (11, 26). In those studies, when endocytosis of apoA-I was blocked by pharmacological reagents, there was a concomitant inhibition of cholesterol efflux to apoA-I. apoA-I internalization therefore was thought to be one of the required elements for cholesterol efflux. However, these pharmacological reagents are nonspecific and have multiple known effects on cell functions (28, 29). To avoid this issue, we have developed a protocol that removes surface-bound apoA-I with high specificity and

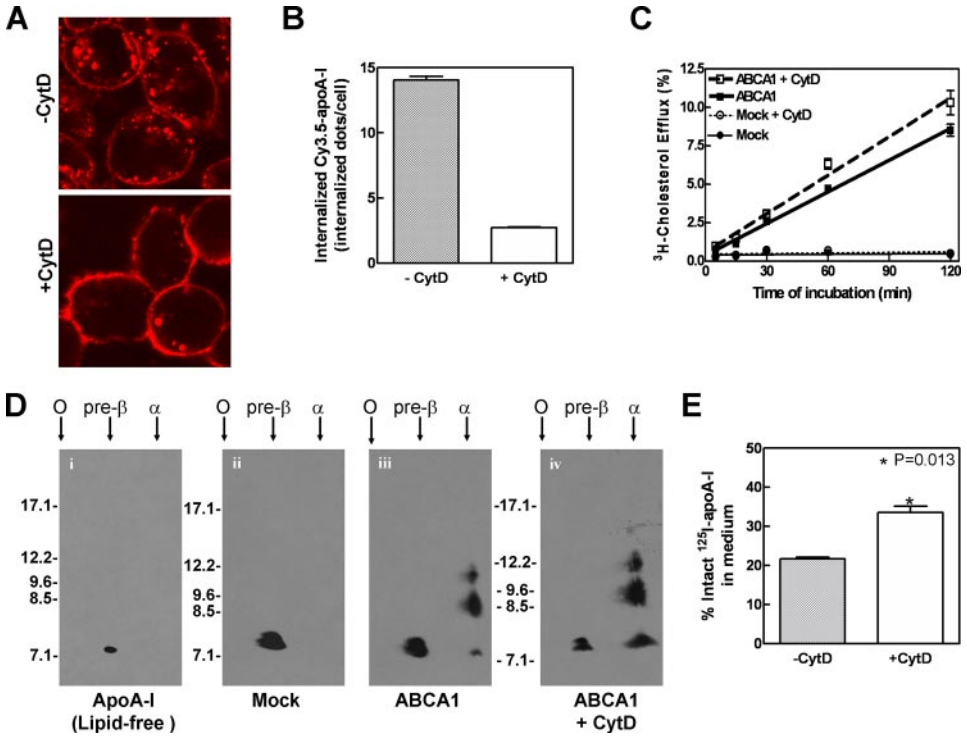

FIGURE 6. **Blocking endocytosis does not impair cholesterol efflux or HDL biogenesis.** *A*, ABCA1-expressing BHK cells were preincubated for 15 min without or with 6 μM cytochalasin D (*CytD*) to inhibit endocytosis. The cells were then pulse-labeled for 5 min with 5 μg/ml Cy3.5-apoA-I and chased for 120 min in the presence or absence of cytochalasin D. Cy3.5-apoA-I was visualized by confocal microscopy. *B*, internalized Cy3.5-apoA-I was quantified by counting cytosolic dots per cell. The data represent the means ± standard deviation among ~130 individual cells. *C*, [^{3}H]cholesterol-labeled induced cells were preincubated in DMEM with or without 6 μM cytochalasin D for 15 min. Cholesterol efflux was performed by incubation with 5 μg/ml of apoA-I with or without 6 μM cytochalasin D for 2 h. *D*, 2-h efflux medium was collected for each condition and subjected to nondenaturing two-dimensional gel electrophoresis followed by immunoblotting against apoA-I. Lipid-free apoA-I incubated without cells (*panel i*) or incubated with mock BHK (*panel ii*) remained unlipidated and migrated at a pre-β position because it failed to generate nascent HDL particles. *E*, blocking endocytosis increased the proportion of trichloroacetic acid-precipitable intact ^{125}I-apoA-I in the medium after 1 h of chase.

efficiency. This allowed us, for the first time, to dissect the contribution of internalized and surface-bound apoA-I to HDL formation in unperturbed cells. The kinetic parameters from these biochemical analyses indicate a rather minor contribution of resecreted apoA-I to HDL generation. Interestingly, we also used two pharmacological reagents (cytochalasin D and sucrose) that block apoA-I endocytosis but found no effect on cholesterol efflux. This highlights the difficulties in interpreting observations obtained using pharmacological inhibitors.

Our results show that apoA-I rapidly dissociates from the plasma membrane to form HDL. A similar dissociation of apoA-I from the membrane inside the endosome could explain why internalized apoA-I was eventually targeted to the lysosomes. We observed that, although initially membrane-bound, internalized apoA-I did not follow the membrane recycling pathway as other membrane-bound proteins, such as Tf. Instead, apoA-I followed the bulk lumen marker dextran. This indicates that apoA-I must have rapidly dissociated from the membrane after internalization and appeared in the lumen of the endosomes. The dissociation could be due to increasing acidity in the endosomes, similar to the dissociation of low density lipoprotein from its receptor (30). This is, however, unlikely because the apoA-I/membrane association was unaffected by acid washing. Alternatively, apoA-I may acquire lipids and thus dissociate into the lumen of the organelle leading to its lysosomal delivery. The rapid lipidation of apoA-I in the endocytic pathway therefore likely contributes to its lysosomal destination and, by doing so, largely excludes it from participating in the production of HDL.

We show that internalized apoA-I did not significantly colocalize with ABCA1, consistent with recent studies showing that only a minor fraction of apoA-I is bound to ABCA1 (21, 22). By remaining bound to ABCA1, apoA-I may undergo receptor-mediated endocytosis. The apoA-I·ABCA1 complex would then recycle back to the cell surface, thereby protecting both apoA-I and ABCA1 from degradation (31).

The BHK-ABCA1 cell model used here admittedly has some limitations. However, we showed here that extracellular lipid-poor apoA-I is rapidly endocytosed and targeted to lysosome in most cell types, including hepatocytes. Although the liver is a major source of HDL *in vivo*, hepatocytes may not depend on extracellular apoA-I lipidation to produce HDL. Indeed, apoA-I has been shown to be secreted as lipidated particles, presumably because of intracellular lipidation along the secretory pathway (32). This process could not be explored in our system. More research will be required to elucidate the relative contribution of the *de novo* secretory pathway *versus* the plasma membrane lipidation pathway in hepatocytes.

To our knowledge, this is the first quantitative analysis of the fate of endocytosed apoA-I. We report that HDL is mainly produced from the plasma membrane, not in the retro-endocytosis pathway. Our results therefore dismiss one of the predominant models in the ABCA1 research field. Interestingly, the conclusions presented here are concordant with a recent report in which apoA-I preferentially interacts with membranes bearing positive curvatures (33), a unique characteristic of the plasma membrane. The search for the molecular mechanism by which ABCA1 generates HDL can now focus on the plasma membrane. More importantly, we can now also hypothesize the importance of the physical properties of the plasma membrane in HDL generation and anticipate new therapeutic strategies to raise HDL *in vivo* by manipulating the plasma membrane.

Acknowledgments—We thank Drs. J. Karwatsky and A. Sorisky for critically reviewing the manuscript.

REFERENCES

1. Bodzioch, M., Orso, E., Klucken, J., Langmann, T., Bottcher, A., Diederich, W., Drobnik, W., Barlage, S., Buchler, C., Porsch-Ozcurumez, M., Kaminski, W. E., Hahmann, H. W., Oette, K., Rothe, G., Aslanidis, C., Lackner, K. J., and Schmitz, G. (1999) *Nat. Genet.* **22,** 347–351
2. Brooks-Wilson, A., Marcil, M., Clee, S. M., Zhang, L. H., Roomp, K., van Dam, M., Yu, L., Brewer, C., Collins, J. A., Molhuizen, H. O., Loubser, O., Ouelette, B. F., Fichter, K., Ashbourne-Excoffon, K. J., Sensen, C. W., Scherer, S., Mott, S., Denis, M., Martindale, D., Frohlich, J., Morgan, K., Koop, B., Pimstone, S., Kastelein, J. J., and Hayden, M. R. (1999) *Nat. Genet.* **22,** 336–345
3. Orso, E., Broccardo, C., Kaminski, W. E., Bottcher, A., Liebisch, G., Drobnik, W., Gotz, A., Chambenoit, O., Diederich, W., Langmann, T., Spruss, T., Luciani, M. F., Rothe, G., Lackner, K. J., Chimini, G., and Schmitz, G. (2000) *Nat. Genet.* **24,** 192–196
4. Rust, S., Rosier, M., Funke, H., Real, J., Amoura, Z., Piette, J. C., Deleuze, J. F., Brewer, H. B., Duverger, N., Denefle, P., and Assmann, G. (1999) *Nat. Genet.* **22,** 352–355
5. Batal, R., Tremblay, M., Krimbou, L., Mamer, O., Davignon, J., Genest, J., Jr., and Cohn, J. S. (1998) *Arterioscler. Thromb. Vasc. Biol.* **18,** 655–664
6. Bojanovski, D., Gregg, R. E., Zech, L. A., Meng, M. S., Bishop, C., Ronan, R., and Brewer, H. B., Jr. (1987) *J. Clin. Investig.* **80,** 1742–1747
7. Fitzgerald, M. L., Morris, A. L., Rhee, J. S., Andersson, L. P., Mendez, A. J., and Freeman, M. W. (2002) *J. Biol. Chem.* **277,** 33178–33187
8. Nofer, J. R., and Remaley, A. T. (2005) *Cell Mol. Life Sci.* **62,** 2150–2160
9. Landry, Y. D., Denis, M., Nandi, S., Bell, S., Vaughan, A. M., and Zha, X. (2006) *J. Biol. Chem.* **281,** 36091–36101
10. Neufeld, E. B., Stonik, J. A., Demosky, S. J., Jr., Knapper, C. L., Combs, C. A., Cooney, A., Comly, M., Dwyer, N., Blanchette-Mackie, J., Remaley, A. T., Santamarina-Fojo, S., and Brewer, H. B., Jr. (2004) *J. Biol. Chem.* **279,** 15571–15578
11. Takahashi, Y., and Smith, J. D. (1999) *Proc. Natl. Acad. Sci. U. S. A.* **96,** 11358–11363
12. Mukherjee, S., Zha, X., Tabas, I., and Maxfield, F. R. (1998) *Biophys. J.* **75,** 1915–1925
13. Mukherjee, S., Ghosh, R. N., and Maxfield, F. R. (1997) *Physiol. Rev.* **77,** 759–803
14. Jing, S. Q., Spencer, T., Miller, K., Hopkins, C., and Trowbridge, I. S. (1990) *J. Cell Biol.* **110,** 283–294
15. Mayor, S., and Pagano, R. E. (2007) *Nat. Rev. Mol. Cell. Biol.* **8,** 603–612
16. Pagano, R. E. (1990) *Curr. Opin. Cell Biol.* **2,** 652–663
17. Vaughan, A. M., and Oram, J. F. (2003) *J. Lipid Res.* **44,** 1373–1380
18. Duong, P. T., Collins, H. L., Nickel, M., Lund-Katz, S., Rothblat, G. H., and Phillips, M. C. (2006) *J. Lipid Res.* **47,** 832–843
19. Krimbou, L., Hajj, H. H., Blain, S., Rashid, S., Denis, M., Marcil, M., and Genest, J. (2005) *J. Lipid Res.* **46,** 1668–1677
20. Neufeld, E. B., Remaley, A. T., Demosky, S. J., Stonik, J. A., Cooney, A. M., Comly, M., Dwyer, N. K., Zhang, M., Blanchette-Mackie, J., Santamarina-Fojo, S., and Brewer, H. B., Jr. (2001) *J. Biol. Chem.* **276,** 27584–27590
21. Hassan, H. H., Denis, M., Lee, D. Y., Iatan, I., Nyholt, D., Ruel, I., Krimbou, L., and Genest, J. (2007) *J. Lipid Res.* **48,** 2428–2442
22. Vedhachalam, C., Ghering, A. B., Davidson, W. S., Lund-Katz, S., Rothblat, G. H., and Phillips, M. C. (2007) *Arterioscler. Thromb. Vasc. Biol.* **27,** 1603–1609
23. Zha, X., Genest, J., Jr., and McPherson, R. (2001) *J. Biol. Chem.* **276,** 39476–39483
24. Luzio, J. P., Pryor, P. R., and Bright, N. A. (2007) *Nat. Rev. Mol. Cell. Biol.* **8,** 622–632
25. Mayor, S., Presley, J. F., and Maxfield, F. R. (1993) *J. Cell Biol.* **121,** 1257–1269
26. Lorenzi, I., von Eckardstein, A., Cavelier, C., Radosavljevic, S., and Rohrer, L. (2008) *J. Mol. Med.* **86,** 171–183
27. Chadda, R., Howes, M. T., Plowman, S. J., Hancock, J. F., Parton, R. G., and Mayor, S. (2007) *Traffic* **8,** 702–717
28. Sieczkarski, S. B., and Whittaker, G. R. (2002) *J. Gen. Virol.* **83,** 1535–1545
29. Sigal, N. H., and Dumont, F. J. (1992) *Annu. Rev. Immunol.* **10,** 519–560
30. Brown, M. S., and Goldstein, J. L. (1986) *Science* **232,** 34–47
31. Wang, N., Chen, W., Linsel-Nitschke, P., Martinez, L. O., Agerholm-Larsen, B., Silver, D. L., and Tall, A. R. (2003) *J. Clin. Investig.* **111,** 99–107
32. Kiss, R. S., McManus, D. C., Franklin, V., Tan, W. L., McKenzie, A., Chimini, G., and Marcel, Y. L. (2003) *J. Biol. Chem.* **278,** 10119–10127
33. Vedhachalam, C., Duong, P. T., Nickel, M., Nguyen, D., Dhanasekaran, P., Saito, H., Rothblat, G. H., Lund-Katz, S., and Phillips, M. C. (2007) *J. Biol. Chem.* **282,** 25123–25130